UNIVERSITÀ DEGLI STUDI DI PADOVA

Dipartimento di Fisica e Astronomia "Galileo Galilei"

Corso di Laurea in Fisica

Tesi di Laurea

Quantum entanglement in High-Energy Physics

Entanglement quantistico nella fisica delle alte energie

Relatrice

Prof.ssa Ramona Gröber

Laureando

Alessandro Baravelli

Anno Accademico 2023/2024

Introduction

Quantum mechanics is at the foundation of modern physics. It introduced several groundbreaking concepts, among which entanglement stands out. This phenomenon describes a deep connection between different parts of a quantum system, where to understand a part fully, information about another is needed, regardless of the distance separating them. This spatial independence highlights the unique and non-intuitive nature of quantum correlations, setting quantum mechanics apart from classical physical theories.
The exploration of entangled states has long been a central theme within atomic and solid-state physics, but it's only in recent times that the high-energy physics field has begun to actively engage with this research area, making it quite a hot topic. In quantum field theory, states are characterized by their mass, momentum, and spin, as they form the irreducible representations of the Poincaré group. However, within the framework of the perturbative S-matrix, calculations are feasible exclusively in momentum space. As a result, entanglement manifests in the spin correlations of particles and must be examined as such. The process of analyzing these correlations to deduce the complete quantum state post-scattering is known as quantum state tomography. As of today, there are multiple reasons that make this exploration relevant:

- It provides a confirmation of the most counter-intuitive phenomenon of quantum mechanics in a new context.
- It gives us a probe of new physics, exploring well-established forces of nature, and possibly new ones.
- The less control over the experimental setup is well balanced by the enormous amount of data collected.

In this thesis, I introduce the concept of quantum entanglement, a few basic ideas related to the standard model of particle physics and three HEP scenarios involving entanglement and/or non-locality. In particular I explore the production of top quarks, the decay of the Higgs boson into leptons and the decay of charmonium. The numerical results are reproduced using software such as python, MadAnalysis5 [1] and MadGraph5_aMC [2].

Chapter 1

Quantum entanglement

1.1 Historical Overview

The word *entanglement* was coined in 1935 by Schrödinger following a paper published months earlier by Einstein, Podolsky, and Rosen [3], commonly known as the EPR paper. Schrödinger was referring to an inherently quantum mechanical effect which the authors used as a proxy to disprove quantum mechanics' completeness. Ironically, this phenomenon would later become a key feature of the theory itself. Following the EPR paper, a few concepts are defined: e.g. a theory is said to be *complete* if to every element of reality an element of the physical theory is assigned, moreover a quantity is said to be *real* if it can be predicted with certainty without disturbing in any way the system. In that regard, it is well known that QM doesn't simultaneously predict the values of two conjugated observables, such as position and momentum. One might argue that these quantities can't be both real, but in the gedankenexperiment they make use of a causality principle to negate such possibility. They imagine two entangled systems, that have interacted in the past, and that are now spatially apart (such that light and information can't be exchanged between the two). Changing the type of measurement conducted on the first one, it is possible to predict with certainty two conjugated quantities of the second one. Mathematically, they describe an entangled state of the kind $|\psi\rangle = \int dp e^{ipx_0}|p\rangle|-p\rangle = \int dx|x+x_0\rangle|x\rangle$, of particles with definite relative position (x_0) and center of mass, where x is the coordinate along the direction of motion. We could say that this state allows multiple bi-orthonormal expansions and different types of measurements on the first system trigger the reduction of the wave packet onto two incompatible states of the second one (from the position of particle A we deduce the position of particle B, likewise for the momentum). By the definition of the authors, these quantities associated with the second particle are *real*, because are predictable with certainty without in any way disturbing the second system, thanks to the causal separation. Yet, QM does not simultaneously define them, thus disproving its completeness. This assumption relies on the local idea that two non-interacting systems can't influence each other's *reality*.

Just two months later, N. Bohr replied to their article with a homonymous paper. As one of the main defenders of quantum mechanics, he attempted to counter their arguments by introducing the concept of **complementarity**. This principle involves the experimentalist's renunciation of knowledge about one physical quantity due to the act of measuring another. However, this argument did not convince the authors of the EPR paper and failed to address their main concern. Ironically, Bohr was a harsh critic of many last-century scientific breakthroughs, including Einstein's photon, Schrödinger's equation, Dirac's equation, the neutrino, and pions.

In an article published by J.S.Bell [4] in 1964 it is clearly shown that adding additional parameters to restore QM locality would not reproduce the high level of correlation predicted by the theory. The original example is that of two spin one-half ($\vec{\sigma_1}$ and $\vec{\sigma_2}$) particles in a singlet state moving freely in opposite directions. Being $\vec{a}$ and $\vec{b}$ two possible orientations of the spin measurement, the quantum theory predicts $P(\vec{a},\vec{b}) = \langle(\vec{\sigma_1}\cdot\vec{a})\cdot(\vec{\sigma_2}\cdot\vec{b})\rangle = -\vec{a}\cdot\vec{b}$. This value is a representation of the correlation between the two spins. We could use a parameter λ to describe the hidden variable, which could be continuous or discreet, a scalar or a vector, fixed or with his laws of motion (as intended by Ein-

stein), which means that it is a dynamical variable that evolves. Through a few inequalities it can be proven that the quantum mechanical explanation cannot be represented, either accurately or arbitrarily closely, by a hidden variable perspective. In conclusion, Bell says that in a hidden-variable theory, there must be a mechanism whereby the setting of one measuring device can affect the reading of another instrument, however remote. Such a theory would not be Lorentz invariant. Thus, it becomes crucial to perform experiments in which the settings are changed mid-flight to test QM validity. In quantum information theory, tests of quantum entanglement are often referred to as Bell tests.

1.2 Bell Tests

In the last 60 years, there have been many attempts at confirming the existence of entanglement [5], that *spooky action at a distance* as Einstein used to call it. Many observables have been proposed and studied to partially or completely disprove any hidden-variable theory. These tests are often expressed in the form of an inequality and each one may come at hand for different use cases. In particular, the original one put forward by Bell isn't the simplest to violate in an actual experiment. A more common one is the famous Clauser-Horne-Shimony-Holt inequality, or **CHSH inequality** [6]: two separate Stern–Gerlach devices A and B measure a quantity that can be equal to +1 or -1 (e.g. the spin) over two random directions each (A_1,A_2,B_1,B_2). If we assume realism (the quantities a_i, b_i existing before measurement) and locality (the choices of A_i, B_i have no effect on b_i or a_i respectively) than

$$\langle A_1 B_1 \rangle + \langle A_1 B_2 \rangle + \langle A_2 B_1 \rangle - \langle A_2 B_2 \rangle \leq 2. \tag{1.1}$$

That is because the result of a single measurement (averaged over the possible directions) is $(a_1 + a_2)b_1 + (a_1 - a_2)b_2 = \pm 2$ and the mean over multiple measurements must be in between these values. CHSH-type inequalities exist even at dimensions $d > 2$, possibly infinite [7].
Other noteworthy Bell tests are the class of Greenberger–Horne–Zeilinger experiments or **GHZ experiments** [8], which use three or more entangled particles and give rise to starkly contrasting predictions between QM and local hidden-variable theories. They make an effort to produce a test that doesn't rely on inequalities. An example of the kind is that of three particles in the state given by $|\psi\rangle = \frac{1}{\sqrt{2}}(|\text{-1-1-1}\rangle - |111\rangle)$ where each $|\pm 1\rangle$ is the corresponding eigenstates of σ_z. $|\psi\rangle$ is easily shown to be an eigenstate of every permutation of $\sigma_x \otimes \sigma_y \otimes \sigma_y$ with an eigenvalue equal to 1. If we assume a realist approach and imagine that the result of a spin measurement over every direction $a_x, a_y, a_z, b_x, b_y, c_x, c_y$ is predefined for each particle, we can multiply together the permutations of $a_x b_y c_y = 1$ ($a_y b_x c_y = 1$, $a_y b_y c_x = 1$) and use $a_y^2 = b_y^2 = c_y^2 = 1$ to get $a_x b_x c_x = 1$. Yet, the quantum mechanical prediction for the observable $\sigma_x \otimes \sigma_x \otimes \sigma_x$ is -1. Thus the contradiction.
It is important to notice that while inequalities true in local hidden-variable theories can be violated in quantum mechanics, this violation can't be arbitrarily big. The maximum value of violation of a Bell-type inequality is called *Tsirelson's bound* [9]. In the case of the CHSH inequality (if the variables commute like $[A_i, B_j] = 0$), this limit is equal to $2\sqrt{2}$. We want it to be as large as possible to ease the experimental burden (difficulty of making precise and relevant measurements), putting it differently it would be easier to detect a violation if this violation can be big in the first place. Often, the inequality is expressed using a **Bell operator** B, whose expected value gives the quantity of interest. For example, for CHSH we define

$$B = (\vec{n}_1 \cdot \vec{\sigma}) \otimes [(\vec{n}_2 - \vec{n}_4) \cdot \vec{\sigma}] + (\vec{n}_3 \cdot \vec{\sigma}) \otimes [(\vec{n}_2 + \vec{n}_4) \cdot \vec{\sigma}], \tag{1.2}$$

where n_i are the unit vectors along which we make the measurements and $\vec{\sigma}$ it the vector of Pauli matrices. The expression in eq. (1.2) is based on the correspondence $\langle A_i B_j \rangle = \langle \Psi | (\vec{n}_i \cdot \vec{\sigma}) \otimes (\vec{n}_j \cdot \vec{\sigma}) | \Psi \rangle$, where $\vec{n} \cdot \vec{\sigma}$ is the spin observable along a specific direction $\vec{n}$.
It is quite relevant to poise on the hierarchy of quantum correlation phenomena. Indeed, the violation of Bell inequalities is just a sufficient but not necessary condition for entanglement. In summary,

$$\text{Bell inequality violation} \subset \text{Entanglement} \subset \text{Quantum correlations} \subset \text{Classical correlations}. \tag{1.3}$$

Entanglement loopholes

One needs to be aware of loopholes, or ways that quantum mechanical results may be misleadingly reproduced. The most common ones are the following

- **Detection Loophole**: Arises when not all entangled particles are detected, potentially biasing the sample towards more detectable events and misrepresenting the strength of entanglement.
- **Locality Loophole**: Occurs if the measurement on one particle could influence the outcome on the entangled partner, violating the principle that these measurements should be causally disconnected.
- **Memory Loophole**: Suggests that successive measurements on entangled particles are not independent, with particles *remembering* previous measurements and adjusting their behavior, which could falsely suggest quantum correlations.
- **Coincidence Loophole**: Involves incorrectly identifying or pairing the measurement outcomes of entangled particles, leading to inaccurate conclusions about correlations.
- **Super-determinism**: Proposes that all events, including choices of measurement settings, are predetermined, thus challenging the foundation of free will assumed in Bell tests.

During the years, many of these backdoors have been closed, especially at low energies. Aspect in 1982 performed the first experimental test following Bell's initial suggestion about space-like separation [10]. Even though his results, and many thereafter, have been found inconsistent with local realism, only in 2015 a (practically) loophole-free Bell test was executed [11]. Aspect claimed that no test can be considered completely loophole-free, as there are explanations of the observations that can't be tested such as superdeterminism, but that reasonable hidden variable theories can now be excluded.

1.3 Mathematics of entangled states

In quantum mechanics, a particle is completely described by its state, denoted as $|\psi\rangle$, which is a vector ray in an appropriate Hilbert space. When expressing this state in the framework of generalized position eigenstates with the projection $\langle\Psi|x\rangle$, we obtain the more familiar wave function $\Psi(x)$. To complete the picture we could consider another intrinsic property of the particle: its spin along a specified direction. This corresponds to a Hilbert space of dimension $2s+1$ and mathematically the state vector has to live in the tensor product space between the spatial and spin component. The same reasoning applies in the presence of more than one particle, where a Hilbert space H_i is associated with each of the particles and the system state is simply $|\psi\rangle = |\psi_1\rangle \otimes |\psi_2\rangle$ and it is an element of $H_1 \otimes H_2$. Yet, it is not always possible to do the inverse or write a generic state of two particles in $H_1 \otimes H_2$ as a tensor product. A pure state for which it is possible is called *separable*. In the opposite case, states are referred to as *entangled*. Later it will become clear as to why this develops into the properties explored before. For a pure or maximally known state, a simple indicator of entanglement is the Schmidt rank. It is equal to the total number of coefficients, counted with multiplicity, in the Schmidt decomposition $|\psi\rangle = \sum_i^m \alpha_i |\phi_i\rangle \otimes |\chi_i\rangle$ where $|\phi_i\rangle_m$ and $|\chi_i\rangle_n$ are respectively orthonormal basis of H_1 and H_2, with dimension $m \leq n$. Moreover, the coefficients α_i can be shown to be real, non-negative, and unique up to reordering.

It is now useful to introduce the concept of the *density matrix*, which allows us to describe a system not maximally known. This is often the case in experimental physics, where the observations are over an ensemble of events. If the state is thus a statistical mixture of the kind $\{(|\psi_k\rangle, p_k)\}_k$, where p_k are classical probabilities, we define

$$\rho = \sum_k p_k |\psi_k\rangle\langle\psi_k| \tag{1.4}$$

This operator holds relevant physical information and has very useful properties:

- Hermitian: $\rho = \rho^\dagger$ (Hermitian conjugate), implying real eigenvalues.

- Positivity: All eigenvalues of ρ are non-negative.
- Trace: $\mathrm{Tr}(\rho) = 1$, indicating that the probabilities sum to one.
- Expectation Values: Expectation values of observables A are given by $\langle A \rangle = \mathrm{Tr}(\rho A)$.
- Basis Independence: The density matrix representation is basis-independent.
- Purity: The purity of a state is given by $\mathrm{Tr}(\rho^2)$ and ranges from 0 (completely mixed) to 1 (pure state).

The collection of density matrices that describe a quantum system constitutes a convex subset. This arises because any convex combination of density matrices, also forms a density matrix. Pure states stand as the extremal points of this subset, meaning they cannot be depicted as convex combinations of other density matrices. These pure states are fundamental in decomposing non-pure states, thereby generating the entire set of density matrices. Given a set of positive operators satisfying $\sum V_i V_i^\dagger = I$, we can call a **quantum channel** or quantum operation [12] the linear map over the space of density matrices given by

$$\rho \to E[\rho] = \sum_i V_i \rho V_i^\dagger$$

A trivial quantum channel is given by the Hamiltonian unitary evolution, defined as $V = e^{-\frac{i}{\hbar}Ht}$.
If the system is composite, we define the reduced density matrix relative to the first subsystem $\rho_1 = \mathrm{Tr}_2(\rho)$, obtained by taking the partial trace with respect to the base of the second one. A noteworthy possibility is that the resulting reduced matrix represents a mixed state, even though the initial state was pure. A necessary and sufficient condition for the initial state to be separable is that the purity of the state is conserved after taking the partial trace. This criterion is not particularly useful, because we rarely start with a pure state in the first place.

1.4 Separability problem

In general, it is not an easy task to determine whether a given density matrix describes a separable or an entangled state, we may refer to it as the *separability problem*. In particular, we have not yet identified a necessary and sufficient condition for the separability of a bipartite system with arbitrary dimension, as is the focus of the cases explored hereafter. Nevertheless, we cannot hope to change the locality of a state by only performing local operations and classical communication (**LOCC** for short), of the kind $O_A \otimes O_B$, where O_i is a positive map. Measures of entanglement that are non-negative and do not increase under LOCC are called **entanglement monotones**.

Positivity violation

From this simple idea we get an immediate **entanglement witness** (i.e. a quantity that gives sufficient conditions for entanglement).

$$\begin{aligned} &\text{A bipartite system } \rho \text{ is classified as entangled if and only if there exists a positive map } \Lambda_A \\ &\text{acting on the subsystem } S_A, \text{ such that the resulting matrix } \rho \\ &\text{is not positive semi-definite after the application of the combined map } \Lambda_A \otimes I_B, \\ &\text{or } (\Lambda_A \otimes I_B)[\rho] \not\succeq 0. \end{aligned} \tag{1.5}$$

Being this condition theoretically sound, from an experimental perspective not all positive maps have physical significance.

Peres-Horodecki Criterion

The criterion, also known as *Positive Partial Transpose* criterion (PPT), states that:

$$\text{If } \rho \text{ is separable, then its partial transpose } \rho^{T_B} \text{ has non-negative eigenvalues.} \tag{1.6}$$

Here, ρ^{T_B} denotes the partial transpose of ρ with respect to system B and it is just an application of the previous witness. The proof of this necessary condition for separability is straightforward. Indeed, given a separable state, it can be written as $\rho = \sum p_i \rho_i^A \otimes \rho_i^B$. After the partial transposition we simply get $\rho^{T_B} = \sum p_i \rho_i^A \otimes (\rho_i^B)^T$. But because this operation preserves eigenvalues, we have that $(\rho_i^B)^T$ is still positive semi-definite. The PPT criterion can be shown to be also a sufficient condition for the two-qubits ($2 \otimes 2$ dimension) and qutrit-qubit ($3 \otimes 2$) cases. We can also quantify the entanglement by defining the **negativity**, that is the sum of all the negative eigenvalues of the partially transposed density matrix [13].

Entropy of Entanglement

In classical information theory, Shannon entropy measures the level of uncertainty or surprise associated to a variable's possible outcomes. For a discrete random variable $X : \Omega \to \mathcal{X}$ that induces the probability density $p : \mathcal{X} \to [0, 1]$, Shannon entropy is defined as $H = -\sum_{x \in \mathcal{X}} p(x) \log p(x)$. The natural extension of Shannon entropy for quantum information is Von Neumann's [12], which is defined as $-\mathrm{Tr}(\rho \log \rho)$ and describes the uncertainty we have about the state of the system, or likewise the expected update in information we would get by performing a measurement. Because the trace is invariant over a change of basis, this definition is equivalent to stating $H = -\sum \eta_i \log \eta_i$ where η_i are the eigenvalues of ρ. This means that the expression is equivalent to Shannon entropy, when expressed in the appropriate orthonormal basis. We also deduce that a pure state has an null entropy, because the density matrix is idempotent and each eigenvalue equals one. Given two subsystems A and B, than a measure of entanglement is given by $-Tr(\rho_A \log \rho_A) = -Tr(\rho_B \log \rho_B)$. A pure state is entangled if and only if this value is different from 0. For mixed state we get the following condition

$$\text{If the state } \rho \text{ is separable, than } S[\rho] \geq S[\rho_A] \tag{1.7}$$

This inequality is related to a feature of quantum formalism already noted by Schrodinger in 1935: full knowledge on a system does not imply full knowledge of its parts. In the presence of entanglement, the entropy (i.e. the uncertainty) could increase when considering the subparts of an ensemble.

Concurrence

Concurrence is an entanglement monotone defined for a pure bipartite state as

$$C_A(\rho) = \sqrt{2(1 - \mathrm{Tr}\rho_A^2)} \tag{1.8}$$

Concurrence is mostly useful due to its computational simplicity.

1.5 Qubit-Qubit System

The state of two spin-1/2 particles can be described by a 4 by 4 complex-valued density matrix. It can be decomposed in the following sum

$$\rho = \frac{1}{4}\left[\mathbb{I}_2 \otimes \mathbb{I}_2 + \sum_{i=1}^{3} B_i^+ (\sigma_i \otimes \mathbb{I}_2) + \sum_{i=1}^{3} B_i^- (\mathbb{I}_2 \otimes \sigma_i) + \sum_{i,j=1}^{3} C_{ij} (\sigma_i \otimes \sigma_j)\right] \tag{1.9}$$

where σ_i are the Pauli matrices. In this expression, the values $B_i^+ = \mathrm{Tr}\left[\rho(\sigma_i \otimes \mathbb{I}_2)\right]$, B_i^- and C_{ij} are real, being the expected values of some spin observable. The latter are evidently an expression of the

classical and quantum correlations between the two. While ρ being automatically normalized (indeed we have $16-1=15$ degrees of freedom), the positivity is not guaranteed, and needs to be enforced separately: this limits the range of possible values. An example of this kind of decomposition is given by the pure singlet state

$$|\Psi\rangle = \frac{1}{\sqrt{2}}\left(|\uparrow_{\vec{n}}\rangle \otimes |\downarrow_{\vec{n}}\rangle - |\downarrow_{\vec{n}}\rangle \otimes |\uparrow_{\vec{n}}\rangle\right) \Longrightarrow C_{ij} = -\delta_{ij}$$

along any particular direction $\vec{n}$. In such a framework, the CHSH inequality is expressed by the **Horodecki criterion** [14].

The bipartite spin state ρ described in eq. (1.9) contradicts the CHSH inequality (1.1) if and only if the sum of the two largest eigenvalues of the matrix $M = CC^{\mathsf{T}}$ exceeds 1,

$$m_{12} \equiv m_1 + m_2 > 1. \tag{1.10}$$

Equivalently, there exist a particular choice of $\vec{n_i}$ (i.e. the directions of measurements) such that, given the Bell operator defined in 1.2, we get

$$|\mathrm{Tr}(\rho B)| = |\vec{n_3}\cdot C\cdot(\vec{n_2}-\vec{n_4}) + \vec{n_1}\cdot C\cdot(\vec{n_2}+\vec{n_4})| > 2. \tag{1.11}$$

1.6 Qutrit-Qutrit System

The description of a spin 1/2 particle coincides with the SU(2) symmetry group. Exactly the same can be said for a spin 1 particle with SU(3). The Lie algebra associated with the latter has dimension 8 (instead of 3 for SU(2)) and there are different choices for the generators that can be made.

Gell-mann matrices

These are a set of eight linearly independent 3×3 traceless Hermitian matrices, i.e. λ_i. They are quite often used in physics of the fundamental interaction for the description of the strong force. Importantly, they are a simple generalization of the Pauli matrices. Peculiar is their orthonormality condition, which reads $\lambda_i\lambda_j = 2\delta_{ij}$.

The irreducible tensor operator parametrization

Another way of describing the system is by the combination of cross products $T^{M_1}_{L_1}\otimes T^{M_2}_{L_2}$ of operators whose definition depends on the spin-1 components J_x, J_y, J_z as follows

$$T_1^{\pm} = \mp\frac{\sqrt{3}}{2}(J_x \pm iJ_y) \quad T_1^0 = \sqrt{\frac{3}{2}}\,J_z \tag{1.12}$$

$$T_2^{\pm 2} = \frac{2}{\sqrt{3}}(T_1^{\pm})^2 \quad T_2^{\pm 1} = \sqrt{\frac{2}{3}}\left(T_1^{\pm}T_1^0 + T_1^0T_1^{\pm}\right) \quad T_2^0 = 1frac\sqrt{2}3\left(T_1^{-1}T_1^{+1} + T_1^{+1}T_1^{-1} + 2(T_1^0)^2\right).$$

In matrix form they read

$$J_x = \frac{\hbar}{\sqrt{2}}\begin{pmatrix}0&1&0\\1&0&1\\0&1&0\end{pmatrix} \quad J_y = \frac{\hbar}{\sqrt{2}}\begin{pmatrix}0&i&0\\-i&0&i\\0&-i&0\end{pmatrix} \quad J_z = \hbar\begin{pmatrix}-1&0&0\\0&0&0\\0&0&1\end{pmatrix} \tag{1.13}$$

$$
\begin{aligned}
T_1^+ &= -\hbar\sqrt{\frac{3}{2}}\begin{pmatrix}0&1&0\\0&0&1\\0&0&0\end{pmatrix} & T_1^- &= \hbar\sqrt{\frac{3}{2}}\begin{pmatrix}0&0&0\\1&0&0\\0&1&0\end{pmatrix} & T_1^0 &= \hbar\sqrt{\frac{3}{2}}\begin{pmatrix}1&0&0\\0&0&0\\0&0&\text{-}1\end{pmatrix}\\
T_2^{+2} &= \hbar^2\sqrt{3}\begin{pmatrix}0&0&1\\0&0&0\\0&0&0\end{pmatrix} & T_2^{-2} &= \hbar^2\sqrt{3}\begin{pmatrix}0&0&0\\0&0&0\\1&0&0\end{pmatrix} & & \\
T_2^{+1} &= \hbar^2\sqrt{3}\begin{pmatrix}0&1&0\\0&0&\text{-}1\\0&0&0\end{pmatrix} & T_2^{-1} &= \hbar^2\sqrt{3}\begin{pmatrix}0&0&0\\\text{-}1&0&0\\0&1&0\end{pmatrix} & T_2^0 &= \frac{\hbar^2}{\sqrt{2}}\begin{pmatrix}\text{-}1&0&0\\0&2&0\\0&0&\text{-}1\end{pmatrix}.
\end{aligned}
\tag{1.14}
$$

Clearly, they are a generalization of the bi-dimensional rising and lowering operators for SU(2). The normalization is such that $\mathrm{Tr}(T_M^L(T_M^L)^\dagger) = 3$. Using these operators, the generic density matrix can be written as

$$
\rho = \frac{1}{9}\left[I_3 \otimes I_3 + A_{LM}^1 T_L^M \otimes I_3 + A_{LM}^2 I_3 \otimes T_L^M + C_{L_1M_1L_2M_2} T_{L_1}^{M_1} \otimes T_{L_2}^{M_2}\right] \tag{1.15}
$$

In order for ρ to be Hermitian, the coefficients must satisfy $A_{LM}^{1,2} = (-1)^M (A_{L,-M}^{1,2})^*$ and $C_{L_1M_1L_2M_2} = (-1)^{M_1+M_2}(C_{L_1,-M_1,L_2,-M_2})^*$. These sum up to 80 independent real parameters. This decomposition allow for an easier extraction of the relevant information from the angular distributions of the final leptons, as I will explore in the next chapters.

Chapter 2

High-Energy Physics

High-energy physics is the science that studies elementary particles and the fundamental forces. It aims to understand the underlying principles that describe nature at the smallest scales, an endeavor inevitably associated with high resolution, short wavelengths, and high energy. We could say, somewhat artificially, that the beginning of the **classical era** dates back to 1897, when Thomson discovered the electron by observing cathode rays, and it ends in 1932, with Chadwick's discovery of the neutron completing the picture. Since then, many new discoveries have taken place, expanding our understanding far beyond that initial framework. Though, at that particular moment in time, it seemed remarkably clear what constitutes ordinary matter.

The Standard Model

In the following years, many more particles were discovered, particularly through the detection of cosmic rays, making it increasingly challenging to organize them into a simple, efficient, and revelatory scheme. As the 1955 Nobel winner Willis Lamb [15] humorously suggested:

> "*The finder of a new elementary particle used to be rewarded with a Nobel Prize, but such a discovery now ought to be punished with a $10,000 fine.*"

Noteworthy is the discovery of the photon (proposed by Planck as an emission phenomenon and then generalized by Einstein as an intrinsic property of light itself), the pion (recognized by Yukawa as the mediator of the strong force between nucleons), strange particles (such as the neutral K and Λ, also known as V particles due to the shape their decay products make), quarks (which Gell-Mann predicted with his Eightfold Way), and intermediate vector bosons. The developments in theoretical physics led to the modern Standard Model, a collection of related theories such as QED, the Glashow-Weinberg-Salam theory of electroweak processes, and QCD. This assortment became *orthodoxy* in 1978 [16], meeting every experimental test ever since. Moreover, this theory features an elegant and pleasing aesthetic principle: the need for *local gauge invariance*. Summarizing, the Standard Model describes a total of 61 particles, organized into the following families:

- 36 **quarks**, fermions existing in 6 flavors (up, down, charm, strange, top, bottom), 3 colors (historically RGB) or anticolors (for the antiparticles), and 2 choices of electric charge (positive $+\frac{2}{3}$ or negative $-\frac{1}{3}$). Given the *color neutrality rule*, at low energies these bind together to form hadrons: 9 mesons, 8 baryons, and 8 anti-baryons, plus their excited states.
- 8 **gluons**, massless bosons that mediate the strong force. They are bi-colored and satisfy the same confinement rule as quarks (e.g. glueballs).
- 12 **leptons**, fermions diversified in 3 flavors and electric charge (positive, negative, or neutral). The precise count assumes the existence of Dirac's neutrino, or two kinds of neutral leptons for each flavor (the neutrino and its anti-particle).
- 1 **photon**, the boson mediator of the electromagnetic force.

- 3 **intermediate vector bosons**, massive mediators of the weak force.
- 1 **Higgs boson**, responsible for the masses of elementary particles. Despite being predicted some time ago in 1964 by Peter Higgs [17], it was detected just in 2012 at LHC [18]. It is one of the greatest theoretical predictions of this framework.

The Standard Model, however, requires the empirical calibration of 20 parameters: the masses of quarks and leptons; three angles and a phase in the Cabibbo-Kobayashi-Maskawa (CKM) matrix for the inter-generational quark coupling (the angles are analogs of the Euler angles in 3D rotation, and the phase introduces CP violation); and the Weinberg angle, which is related to the masses of the intermediate vector bosons. Moreover, gravity gets completely ignored due in part to its weakness (which makes it negligible in most subatomic processes). The search for a candidate particle for dark matter also remains a hot topic. It is anticipated that the model will be expanded in the future to accommodate these unknowns (e.g., Grand Unified Theories (GUTs), string theory). However, as of today, there is no experimentally confirmed extension [19].

Feynman diagrams

Scattering and decay processes are often depicted using Feynman diagrams, where time flows from the left to the right while the vertical axis does not represent anything physical. Antiparticles are distinguished by particles through a time reversal convention. Every such diagram results from the composition of more interaction vertices (Fig. 2.1). One diagram can be twisted or rotated to represent more than one process, this reflects the fact that they share the same kind of equations. It is important to clarify that the only observables are the incoming and outgoing particles. Every completion of the inner graph is not just a possibility, but a necessity. However, from the order of the diagram (i.e. the number of vertices) we infer the contribution of a particular graph to the total cross section. For example, in QED each vertex contributes with a factor of α to the cross section associated with a particular diagram, so it is always diminishing (i.e. the more vertices, the more suppression). This property is apparent in QED and less obvious for the strong force, due to a constant greater than one at low energies. As the coupling constants run with the energy scale, QCD becomes perturbative at high energies, i.e. the cross section can be evaluated making use of perturbation theory with the dominant contribution being the simplest tree-level diagram.

QED interaction vertex

Bhabha scattering

Figure 2.1: From an interaction vertex to a physical process

2.1 Kaon mixing and oscillations

Due to quantum superposition, it is not straightforward or even necessary to define exactly what constitutes a particle in itself. Kaons, neutral pseudo-scalar mesons, are often cited as an example. They are usually produced via the strong interaction in pairs as eigenstate of flavor (i.e. strangeness), called K^0 and K^0 and decay through the weak interaction as **approximate** eigenstate of CP, called K_L and K_S. One might argue that the latter are the real particles, having a well defined and exponential decay time. This conversion can happen due to the flavour changing kaon mixing, given by the diagrams in figure 2.2.

Kaon mixing is a topic closely related to CP violation. Indeed, experimental observation suggests

Figure 2.2: Strange oscillation diagrams

that K_L might decay in 2 pions, with a CP eigenvalue equal to 1. This suggests that either we have a direct CP violation or K_L is not exactly an eigenstate of CP, which would entail a violation in itself. Different experiments showed that both hypotheses are actually true. Indeed, if we call K_+ and K_- the effective eigenstates of CP then

$$|K_\pm\rangle = \frac{1}{\sqrt{2}}(|K^0\rangle \pm |\bar{K}^0\rangle) \quad \longrightarrow \quad |K_L\rangle = \frac{1}{\sqrt{1+\epsilon^2}}(|K_+\rangle + \epsilon|K_-\rangle)$$

where ϵ is the **CP violation parameter**. Many experiments have been conducted to also study CPT and T violations. For our purposes, a notable feature of a kaon system is **strange entanglement** and its decoherence. The latter is modelled by the so called master equation and will be explored in the following chapter. Kaon mixing can be easily described by the time-dependent Schrödinger equation, with an Hamiltonian that can be written as

$$i\hbar\frac{\partial}{\partial t}|\Psi(t)\rangle = H|\Psi(t)\rangle \quad H = M - \frac{i}{2}\Gamma \tag{2.1}$$

M and Γ are both hermitian matrices with a constant diagonal. H needs not to be unitary, because we want to account for the decay of the particle itself. In particular, the eigenstates of H are K_L and K_S and they evolve exponentially as such

$$\begin{cases} H|K_S(t)\rangle = (m_S - i\frac{\hbar}{2}\Gamma_S)|K_S(t)\rangle \\ H|K_L(t)\rangle = (m_L - i\frac{\hbar}{2}\Gamma_L)|K_L(t)\rangle \end{cases} \tag{2.2}$$

where the state widths are defined as $\Gamma = \frac{1}{\tau}$ (decay rates of each particle) and are related to the intrinsic uncertainty on the rest energy due to the uncertainty principle. From this, we can derive quite simply the shape of the oscillations in the probability space. The function is drawn in Fig. 2.3, with a survival amplitude given by

$$\left|\langle K^0|K^0(t)\rangle\right|^2 = \frac{1}{4}\left(e^{-\Gamma_S t} + e^{-\Gamma_L t} + 2e^{-\frac{1}{2}(\Gamma_S+\Gamma_L)t}\cos\left(\frac{(m_L - m_S)t}{\hbar}\right)\right) \tag{2.3}$$

Moreover, due to the shorter lifetime of K_S, the fraction of K_L progressively increases inside a beam of neutral kaons, however originally composed. Yet, when the beam travels through matter it exhibits a process of regeneration and loss of coherence, due to the different kinds of interaction possible for K^0 and $\bar{K}^0$. While the first undergoes quasi-elastic scattering with the nuclei, the latter participates in the formation of hyperons (baryons containing at least one strange quark).

Basis in quasi-spin space

We can treat the two strangeness eigenstates K^0 and $\bar{K}^0$ as members of a quasi-spin doublet, respectively $\begin{pmatrix}1\\0\end{pmatrix}$ and $\begin{pmatrix}0\\1\end{pmatrix}$. In this framework, every operator acting on the kaons can be expressed in terms of the Pauli matrices.

$$\begin{cases} \text{-}\sigma_x & \Longleftrightarrow & \text{CP operator} \\ \sigma_y & \Longleftrightarrow & \text{CP violation operator} \\ \sigma_z & \Longleftrightarrow & \text{strangeness operator} \end{cases} \tag{2.4}$$

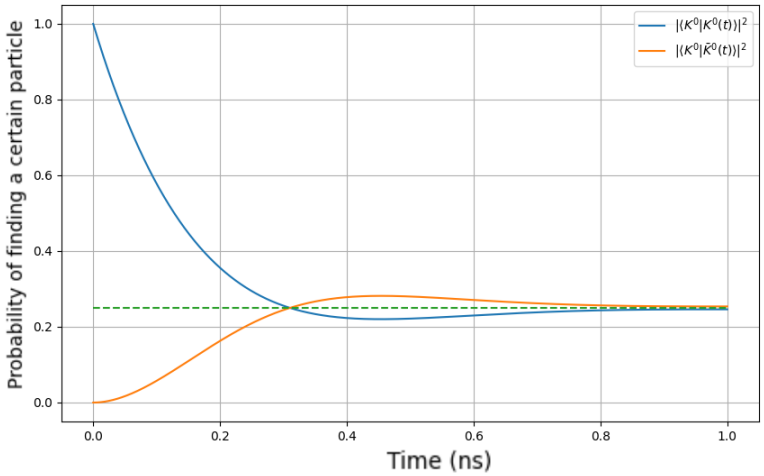

Figure 2.3: Kaons oscillations for a beam of initially pure K^0.

With this notation it is possible to write the Hamiltonian in (2.1) as

$$H = \alpha I + \beta \left(\sin\theta\sigma_x + \cos\theta\sigma_y\right) \tag{2.5}$$

where $\alpha = \frac{1}{2}\left(m_L + m_S - i(\Gamma_L + \Gamma_S)\right)$, $\beta = \frac{1}{2}\left(m_L - m_S - i(\Gamma_L - \Gamma_S)\right)$ and the phase θ corresponds to the CP parameter ε such that $e^{i\theta} = \frac{1-\varepsilon}{1+\varepsilon}$. Now there are different basis we can use depending on the context:

- The eigenbasis of Strangeness, comprising $\{K^0, \overline{K}^0\}$, is useful in the study of electromagnetic and strong interactions that preserve strangeness. For example, in generation processes such as $e^+e^- \to \phi(1020) \to K^0\overline{K}^0$ and $p\overline{p} \to K^0\overline{K}^0$, as well as the identification of neutral kaons through powerful kaon-nucleon interactions. This basis is characterized by its orthonormality, i.e., $\langle K^0|\overline{K}^0\rangle = 0$.

- The eigenbasis of $\{K_S, K_L\}$, which aligns with weak interaction eigenstates that parallel the CP eigenstates denoted as $|K_1\rangle$ and $|K_2\rangle$. This basis is pertinent for the analysis of kaon propagation in a vacuum and contrasts with the CP basis, which is tailored for the study of weak interaction-induced kaon decay processes. It is defined as quasi-orthonormal since $\langle K_S|K_S\rangle = \langle K_L|K_L\rangle = 1$ and the overlap $\langle K_S|K_L\rangle = \langle K_L|K_S\rangle$ is nominally zero, described by $\frac{\epsilon+\epsilon^*}{1+|\epsilon|^2}$.

- The eigenbasis for interaction with matter, labelled as $\{K'_S, K'_L\}$, is defined for understanding the interactions of neutral kaons transiting a homogenous nucleonic substance, which acts simultaneously as a regenerator and absorber. The behavior within this medium is dictated by the Hamiltonian of the medium, modified by an additional term accounting for strong interactions:

$$H_{\text{medium}} = H - \frac{2\pi\nu}{m_K}\begin{pmatrix} f_0 & 0 \\ 0 & \overline{f}_0 \end{pmatrix} \tag{2.6}$$

  where ν represents the nucleonic density of the medium, m_K is the median mass of the K_S and K_L states, and f_0 alongside $\overline{f}_0$ signify the forward scattering amplitudes for K^0 and $\overline{K}^0$, correspondingly. Apart from a small CP violating correction, we get that the relative contribution of $\bar{K}^0$ on the eigenstate of H_{medium} is equal to $\bar{\rho}$ and $\bar{\rho}^{-1}$, for K_S and K_L respectively, where the dimensionless regeneration parameter ρ is equal to [20]

$$\rho = \frac{\pi\nu}{m_K}\frac{f_0 - \overline{f}_0}{m_L - m_S - \frac{i}{2}(\Gamma_L - \Gamma_S)}, \quad \bar{\rho} = \sqrt{1+4\rho^2} + 2\rho, \quad \bar{\rho}^{-1} = \sqrt{1+4\rho^2} - 2\rho \tag{2.7}$$

  We have two limiting cases:

1. At low matter density: $|K'_S\rangle \to |K_S\rangle$ and $|K'_L\rangle \to |K_L\rangle$
2. At high density: $|K'_L\rangle \to |K^0\rangle$ and $|K'_S\rangle \to |\overline{K^0}\rangle$

T and CPT violations

Neutral kaons system can be exploited to study discreet symmetry breaking such as T, CP and CPT. The latter, being preserved due to the so called **CPT theorem**, implies the breaking of T, which of course needs to be observed experimentally as well. In particular, by producing $K^0\bar{K}^0$ pairs through $\phi-$factories and studying one transition process as a reference, it is possible to study T reversal by exchanging the *in* and *out* states [21]. In the process $\phi \to K^0 + \bar{K}^0$, the products are formed in the singlet state given by

$$|i\rangle = \frac{1}{\sqrt{2}}(|K^0\bar{K}^0\rangle - |\bar{K}^0K^0\rangle) = \frac{1}{\sqrt{2}}(|K_+K_-\rangle - |K_-K_+\rangle) \tag{2.8}$$

where we are making two assumptions: firstly neglecting the direct CP violation which entails the orthogonality of the states $\langle K_+|K_-\rangle = 0$ and secondly we identify the decay particle through the sign of the its semileptonic decay based on the rule $\Delta S = \Delta Q$. The latter associates the variations of charge and strangeness for mesons decaying via the weak interaction, which is known to permit flavour changes (CKM mixing matrix). Using the property of the doubly singlet state, we can construct a $flavor$-tag or CP-tag. Based on the type of decay of one kaon, weak semileptonic ($\pi l + \bar{\nu}$ or $\pi l + \bar{\nu}$) or strong ($\pi\pi$ or 3π), we can infer respectively the flavor or CP state of the other. Here, entanglement is indirectly tested, using it as an efficient tool in the experiments.

Chapter 3

Measurements at colliders

In colliders such as the LHC, we have the privilege of observing phenomena in high-energy regimes through processes like scattering and decay, as well as the production of heavy, albeit short-lived, particles. We deal with different than usual applications of quantum mechanics, in the form of quantum field theory. It is of most importance to study how its extravagant consequences develop, and confirming the presence of entanglement in such experimental conditions establishes the generality of the theory. Moreover, we get the rare opportunity of studying entanglement beyond electromagnetic interactions through processes mediated by the strong and/or weak forces, and systems with more than 2 degrees of freedom, i.e. total spin of 1, such as in the decay products of massive bosons. Quantum entanglement observables can at the same time provide additional sensitivity to new physics [22].

Quantum correlations at colliders usually take the form of spin coupling. It is the aim of quantum tomography to predict and study the density matrix after the scattering process. As of today, we have to infer this properties just from the variation of momenta of the outgoing particles. The same happens in the classical Stern-Gerlach apparatus, where particles deviate based on their spin states. We should notice that these momenta commute, but entanglement still remains accessible. The decay time of the entangled pairs ranges from 10^{-25} s for the top quark and the weak gauge bosons to 10^{-20} s for vector mesons and 10^{-13} s for the τ leptons, which is still well under the time taken for the products of the collision to reach the detector [1] . There, we would assist to a loss of correlation due to the interaction with the atoms of the experimental apparatus. In the case of top quarks, the same ideas apply to hadronization, which *would* happen on a longer timescale of around 10^{-23} s, making it completely irrelevant for our purpose.

3.1 Boosted $t\bar{t}$ pair production

One of the most recent attempts to detect entanglement at the LHC involves the production of top quarks. These quarks are boosted, or moving at relativistic speeds, such that the locality loophole is avoided, and the measurements occur at space-like separated positions. The channel studied is the semi-leptonic one, meaning that one quark decays into two leptons, while the other decays into hadrons. Even though the polarization of the latter is known to be challenging to detect, it is possible to reconstruct the spin density matrix of the system using a sophisticated hadronic polarimeter, in combination with jet substructure techniques and neural network-inspired methods [23]. Moreover, the dilepton channel suffers from lower statistics (6 times lower), the reconstruction is not less difficult and most of the decay events happen in causally connected regions [24]. At LHC top pairs are produced mainly through 3 processes: quark-anti quark annihilation, pair production and gluon-gluon annihilation (diagram 3.1). The production of top quark pairs via the strong interaction is a process that respects both parity (P) and charge-parity (CP) conservation. This means that the parameters in the decomposition of the final density matrix 1.9 are quite simpler: $B_i^+ = B_j^- = 0$ and $C = C^T$. In

[1] The time it takes for the products to reach the detector walls at the speed of light, given a tube size of approximately 1 cm, is about 10^{-11} s.

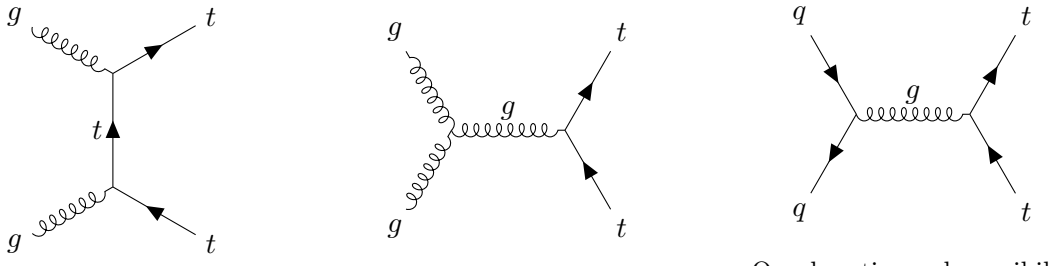

Pair production | Gluon-gluon annihilation | Quark-anti quark annihilation

Figure 3.1: Main $t\bar{t}$ production processes

this scenario, any small deviation caused by the weak force is so minor that they can be ignored. We can now define the following pure and mixed density matrices:

$$\rho^{(\pm)} = |\pm\rangle\langle\pm|\,, \quad |\pm\rangle = \frac{1}{\sqrt{2}}\left(|\uparrow\downarrow\rangle \pm |\downarrow\uparrow\rangle\right), \tag{3.1}$$

$$\rho^{(1)}_{\text{mix}} = \frac{1}{2}\left(|{+}{+}\rangle\langle{+}{+}| + |{-}{-}\rangle\langle{-}{-}|\right), \tag{3.2}$$

$$\rho^{(2)}_{\text{mix}} = \frac{1}{2}\left(|LR\rangle\langle LR| + |RL\rangle\langle RL|\right), \tag{3.3}$$

$$\rho^{(3)}_{\text{mix}} = \frac{1}{2}\left(|\uparrow\downarrow\rangle\langle\uparrow\downarrow| + |\downarrow\uparrow\rangle\langle\downarrow\uparrow|\right), \tag{3.4}$$

where $|\uparrow\rangle$ and $|\downarrow\rangle$ are the eigenvectors of the Pauli matrix σ_z with eigenvalues $+1$ and -1, respectively; similarly, $|\pm\rangle$ are the eigenvectors of σ_x and $|L\rangle$, $|R\rangle$ those of σ_y. We ought to treat a little differently the quark and gluon production mechanisms. It is possible to prove that the state of the $t\bar{t}$ pair is given in the two cases by the convex combinations [25]

$$\rho^{(q\bar{q})}_{t\bar{t}} = \lambda\rho^{(+)} + (1-\lambda)\rho^{(1)}_{\text{mix}}, \quad \text{with} \quad \lambda = \frac{\beta_t^2}{2-\beta_t^2} \in [0,1] \tag{3.5}$$

$$\rho^{(gg)}_{t\bar{t}} = a\rho^{(+)} + b\rho^{(-)} + c\rho^{(1)}_{\text{mix}} + d\rho^{(2)}_{\text{mix}}, \tag{3.6}$$

$$\text{with} \quad a = \frac{\beta_t^4}{1+2\beta_t^2-2\beta_t^4}, \quad b = \frac{(1-\beta_t^2)^2}{1+2\beta_t^2-2\beta_t^4}, \quad c = d = \frac{2\beta_t^2(1-\beta_t^2)}{1+2\beta_t^2-2\beta_t^4}$$

where β_t is the transverse velocity of the products. We see that for the quarks annihilation, at threshold the state is completely mixed and that correlations become dominant only at high transverse momentum. In the other case, the state is maximally entangled in both limit (when β_t approaches 0 or 1). Both this cases must be included when making a comparison with real data, making the state more mixed as a whole. In [27] it was shown that concurrence, as a measure of entanglement, follows

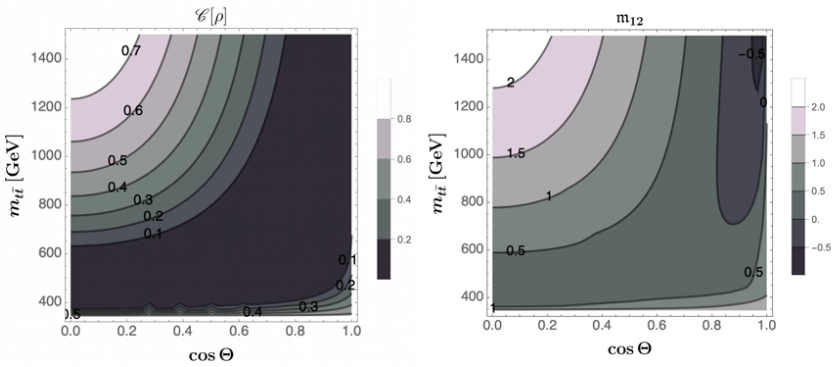

Figure 3.2: Concurrence and m_{12} for top spins, over the whole kinematical space. Image from [26].

the relation

$$C[\rho] = \frac{1}{2}\max(-1-3D, 0), \text{ where } D = \frac{1}{3}\mathrm{Tr}(C). \tag{3.7}$$

Here, $C[\rho]$ is the concurrence defined as in eq. (1.8), while C is the correlation matrix defined in eq. (1.9). Experimentally, it was shown that $D < -\frac{1}{3}$ with a significance over 5σ [28], making it the first evidence of entanglement in top quarks spins. The violation of the Bell inequality can be probed using the Horodecki condition presented in the Chapter 1, in particular I compute the value m_{12}. The violation becomes apparent with the appropriate kinematical conditions, as seen in Fig. 3.2, where θ is the angle of the products of the decay with respect to the transverse direction.

3.2 $H \to ZZ$ decay process

This process suffers from a much lower statistics than the top pair production, especially when we limit ourselves to study the decay of the intermediate vector bosons into one lepton pair each i.e. $H \to ZZ \to e^+e^-\mu^+\mu^-$. Such a selection allows us to easily identify which leptons come from the same parent particle, so that we can compute indirectly its invariant mass. Moreover, this process has also an historical relevance, because the decay into four leptons was one of the main channels through which the Higgs boson was firstly detected. This mainly happened by noticing a bump in the cross section of proton-proton collision with the ATLAS detector, largely due to its excellent momentum resolution [18].

Mathematically, we have to deal with a qutrit-qutrit system, that is because the Z is known to be a spin 1 particle. Moreover, the two bosons are off-shell (virtual), clearly because the some of their rest energies is greater than the mass of the Higgs. For this analysis, we set a frame of reference such that the z-axis is in the direction of the momentum of the Z with the greatest invariant mass, the third component of its spin coincides with the helicity. The density matrix of the joint system is expected to be a 9×9 complex-valued matrix. From symmetry considerations we can reduce the degrees of freedom. A generic pure state in the ensemble needs to conserve the total spin along any particular axis, thus it can be written as the following superposition

$$|\psi\rangle = \alpha_1|+-\rangle + \alpha_2|00\rangle + \alpha_3|-+\rangle \tag{3.8}$$

Moreover, this decay satisfies parity conservation due to how the appropriate Lagrangian term transform under such symmetry. We can limit ourselves to study a state of the type

$$|\psi_{ZZ}\rangle = \frac{1}{\sqrt{2+\beta^2}}(|+-\rangle - \beta|00\rangle + |-+\rangle), \quad \text{with} \quad \beta \in \mathbb{R} \cup \{\infty\} \tag{3.9}$$

The decay has clearly spherical symmetry (in CM frame), thus the value of β can only depend on non trivial kinematical variables such as the invariant masses of the bosons m_1 and m_2, and the modulo of the momentum $|\vec{k}|$. An expression for β can be obtained considering the Lorentz structure of the interaction term $\propto \eta_{\mu\nu} H Z^\mu Z^\nu$ in the SM. Given

$$Z^\mu = \sum_\lambda \frac{d^3\vec{p}}{(2\pi)^3}(a_{p,\vec{\lambda}} e^{-i\vec{p}\cdot\vec{x}} \cdot \epsilon^\mu_\lambda(\vec{p}) + c.c.) \tag{3.10}$$

where $a_{\vec{p},\lambda}$ is called the destruction operator, such that $\tilde{a}_{\vec{p},\lambda}|0\rangle = |\vec{p},\lambda\rangle$ then the state of the ZZ pair is written as

$$|\psi_{ZZ}\rangle = \eta_{\mu\nu}\epsilon^\mu_\sigma(m_1,\vec{k})\epsilon^\nu_\lambda(m_2,-\vec{k})|k,\sigma\rangle|-\vec{k},\lambda\rangle, \tag{3.11}$$

where σ, λ represent spin states and

$$\epsilon^\mu_\sigma(m,\vec{k}) = \begin{pmatrix} 0 & \frac{|\vec{k}|}{m} & 0 \\ -\frac{1}{\sqrt{2}} & 0 & \frac{1}{\sqrt{2}} \\ \frac{i}{\sqrt{2}} & 0 & \frac{i}{\sqrt{2}} \\ 0 & -\frac{\sqrt{|\vec{k}|^2+m^2}}{m} & 0 \end{pmatrix}. \tag{3.12}$$

Comparing eq. 3.9 with eq. 3.11 we get

$$\beta = 1 + \frac{m_H^2 - (m_1 + m_2)^2}{2m_1 m_2} \tag{3.13}$$

From this expression, we see that the larger the mass of the lightest off-shell Z, the less correlations are present. Indeed, for $m_1 + m_2 = m_H$ and $\beta = 1$, we get a maximally entangled state. Meanwhile, for $\beta \to +\infty$ we get a separable state ($|\psi_{ZZ}\rangle = |0\rangle \otimes |0\rangle$). A more precise measure of the expected entanglement is shown in Fig. 3.3. If we ignore noise and other types of contamination, the resulting

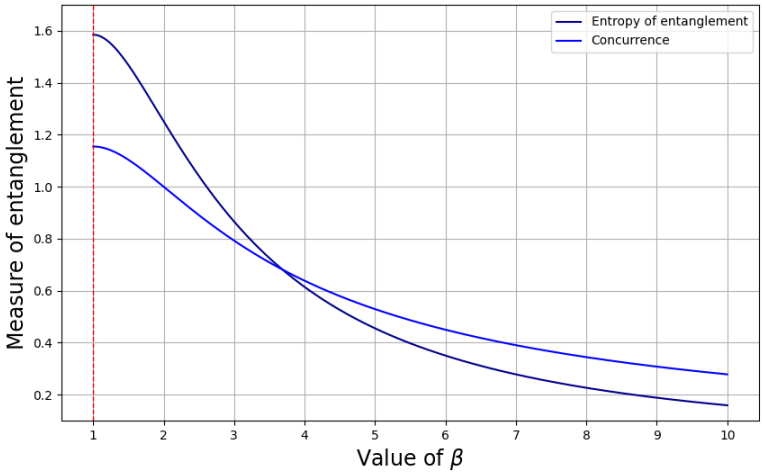

Figure 3.3: Measures of entanglement for the state in eq. (3.9)

density matrix has the following structure, once it has been weighted over different possible pure states.

$$\rho = \frac{1}{2+\omega^2} \begin{pmatrix} 0 & 0 & 0 & 0 & 0 & 0 & 0 & 0 & 0 \\ 0 & 0 & 0 & 0 & 0 & 0 & 0 & 0 & 0 \\ 0 & 0 & 1 & 0 & -y & 0 & 1 & 0 & 0 \\ 0 & 0 & 0 & 0 & 0 & 0 & 0 & 0 & 0 \\ 0 & 0 & -y & 0 & \omega^2 & 0 & -y & 0 & 0 \\ 0 & 0 & 0 & 0 & 0 & 0 & 0 & 0 & 0 \\ 0 & 0 & 1 & 0 & -y & 0 & 1 & 0 & 0 \\ 0 & 0 & 0 & 0 & 0 & 0 & 0 & 0 & 0 \\ 0 & 0 & 0 & 0 & 0 & 0 & 0 & 0 & 0 \end{pmatrix} \tag{3.14}$$

The precise values of w and y in (3.14) depend on the probability distribution functions of β, which internally depends on the physics of the process. Usually it is obtained through Monte Carlo simulations. In particular, I reproduced some previous results [29] using the software MadGraph5_aMC [2] and MadAnalysis5 [1]. The probability distribution function for β is shown in Fig. 3.4.

From a simple fit, we see that the tail follows a power law ($\propto \beta^{-2.87}$), which means the mean value is well-defined. It is now possible to compare the theoretical density matrix with the decomposition in tensor operators introduced in a previous chapter, which simply reads

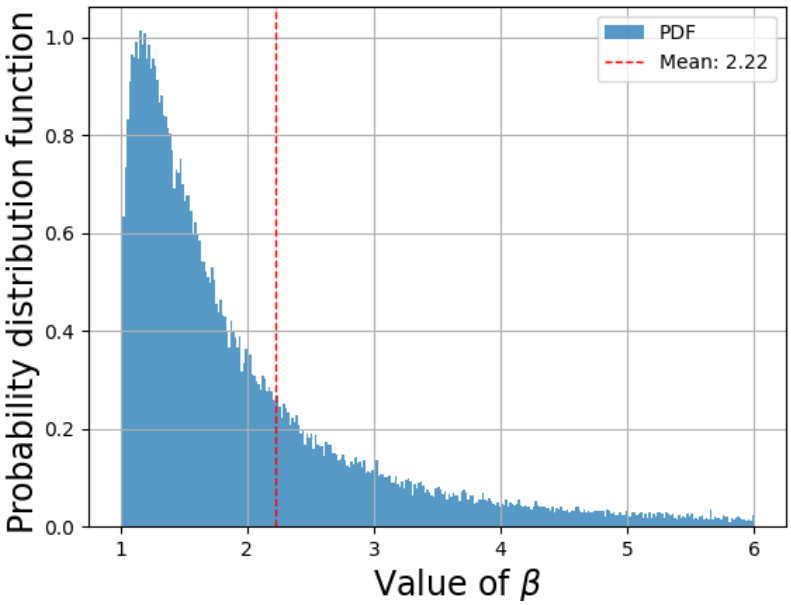

Figure 3.4: Distribution of β obtained with a Monte Carlo simulation.

$$\rho = \begin{pmatrix} 0 & 0 & 0 & 0 & 0 & 0 & 0 & 0 & 0 \\ 0 & 0 & 0 & 0 & 0 & 0 & 0 & 0 & 0 \\ 0 & 0 & \frac{1}{6}\left(\sqrt{2}A_{2,1,0}+2\right) & 0 & \frac{1}{3}C_{2,1,2,-1} & 0 & \frac{1}{3}C_{2,2,2,-2} & 0 & 0 \\ 0 & 0 & 0 & 0 & 0 & 0 & 0 & 0 & 0 \\ 0 & 0 & \frac{1}{3}C_{2,1,2,-1} & 0 & \frac{1}{3}(1-\sqrt{2}A_{2,1,0}) & 0 & \frac{1}{3}C_{2,1,2,-1} & 0 & 0 \\ 0 & 0 & 0 & 0 & 0 & 0 & 0 & 0 & 0 \\ 0 & 0 & \frac{1}{3}C_{2,2,2,-2} & 0 & \frac{1}{3}C_{2,1,2,-1} & 0 & \frac{1}{6}\left(\sqrt{2}A_{2,1,0}+2\right) & 0 & 0 \\ 0 & 0 & 0 & 0 & 0 & 0 & 0 & 0 & 0 \\ 0 & 0 & 0 & 0 & 0 & 0 & 0 & 0 & 0 \end{pmatrix} \tag{3.15}$$

with

$$\text{with} \quad \frac{1}{\sqrt{2}}A^1_{2,0} + 1 = C_{2,2,2,-2} \tag{3.16}$$

The latter expression could be used to estimate the uncertainty and systematics of the experimental apparatus. Intuitively, if more than one coefficient in (3.8) is non-zero, than the state is entangled. This is easily shown by using the Peres-Horodecki criterion. Indeed, taking the partial transpose of a generic density matrix with non-zero entries in the same position as (3.14), we see only positive eigenvalues if the off-diagonal terms are null. As the authors state, this case is one for which we obtain a necessary and sufficient condition for entanglement. The condition for entanglement can also be written as

$$C_{2,1,2,-1} \neq 0 \quad \text{or} \quad C_{2,2,2,-2} \neq 0 \tag{3.17}$$

While it is quite easy to find the optimal Bell operator in the non-relativistic limit ($\beta = 1$), in general one should search in the space of all possible operators for the one that maximizes the violation, a hard endeavor due to the huge parameter space. For slow particles in the state $\frac{1}{\sqrt{3}}(|\text{-}1\text{-}1\rangle + |00\rangle + |11\rangle)$, the right operator has already been found [30] and it can be written as

$$O'_{\text{Bell}} = \frac{4}{3\sqrt{3}}\left(T^1_1 \otimes T^1_1 + T^1_{-1} \otimes T^1_{-1}\right) + \frac{2}{3}\left(T^2_2 \otimes T^2_2 + T^2_{-2} \otimes T^2_{-2}\right) \tag{3.18}$$

For the state at hand, we need to make a little modification in (3.18), and we can just perform a

change of basis as follows

$$O_{\text{Bell}} = (UO_A \otimes U^*)^\dagger O'_{\text{Bell}}(UO_A \otimes U^*) \quad \text{with } O_A = \begin{pmatrix} 0 & 0 & 1 \\ 0 & -1 & 0 \\ 1 & 0 & 0 \end{pmatrix} \tag{3.19}$$

where the choice of the unitary operator U is actually irrelevant. The idea behind this expression is that we can vary U, which cannot be ignored for $\beta \neq 1$, to explore a subset of all possible Bell operators. Even though this strategy could seem a bit crude, it improves the violation well over what would be necessary. In Fig. 3.5 the advantage of the optimal choice becomes apparent, where $I_3 = \text{Tr}(\rho O_{\text{Bell}})$. The trivial identity matrix would not show any significant entanglement (being the vertical dashed line the average of beta over simulated events).

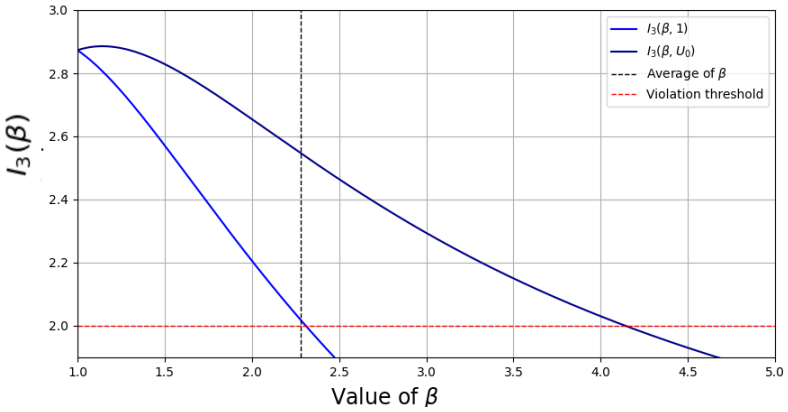

Figure 3.5: Variation of the violation parameter with β, depending on the choice of U

Before performing the actual experiment, it is possible to produce relevant numerical simulations [29]. It has been shown that entanglement can be probed to a significance of 5σ, computing the deviations of $C_{2,1,2,-1}$ or $C_{2,2,2,-2}$ from 0, and the violation of the Bell-type inequality at 4.5σ [29].

3.3 $J/\Psi \to K_S K_S$ decay process

Another relatively straightforward test of non-locality involves the production of neutral kaons through the decay of charmonium [31]. In this analysis, charmonium can be substituted with any vector meson possessing the quantum numbers $J^{PC} = 1^{--}$. Specifically, quantum mechanics predicts that when one particle disintegrates as K_S, the other should collapse into K_L, since the two kaons are produced in a flavor singlet state and $\langle K_S | K_L \rangle \approx 0$ (ignoring CP violations for this discussion). If Einstein's concerns about locality were valid, then it would be possible to observe the process $J/\Psi \to K_S K_S$ in a space-like region.

It is crucial to emphasize that this experimental test does not verify quantum entanglement conclusively because it does not eliminate the possibility of a hidden variable theory. Hence, this test can be interpreted as a confirmation that, under the assumption of the non-existence of hidden variables, quantum mechanics exhibits non-local characteristics.

We can compute the expected amplitude of the $J/\Psi \to K_S K_S$ process assuming locality, namely one kaon must not know the state of the other until the information has had time to travel the appropriate distance. The decay rate can be expressed as

$$\begin{aligned} \Gamma(t_a, t_b)_{\text{non-ent}} \approx \frac{N}{2} \Gamma_L \Gamma_S \{ & e^{-\Gamma_S t_a - \Gamma_L t_b} + e^{-\Gamma_L t_a - \Gamma_S t_b} \\ & - 2\cos((m_L - m_s)(t_b - t_a)) e^{-\frac{1}{2}(t_a + t_b)(\Gamma_S + \Gamma_L)} \} \end{aligned} \tag{3.20}$$

where $N \approx 1.0035$ is a normalization factor, t_i is the proper time of particle i and the blue term is a manifestation of quantum interference, that vanishes after we know that one particle has decayed. If the action at a distance were real, than we would get

$$\Gamma_a(t_a) = \int_0^{t_a} dt_b \, \Gamma_{\text{non-ent}}(t_a, t_b) + \int_{t_a}^{\infty} dt_b \, \Gamma_{\text{ent}}(t_a, t_b) \tag{3.21}$$

$$\Gamma_1(t_1) = 2 \int_{t_1}^{\infty} dt_2 \, \Gamma_{\text{ent}}(t_1, t_2) \tag{3.22}$$

$$\Gamma_2(t_2) = 2 \int_0^{t_2} dt_1 \, \Gamma_{\text{non-ent}}(t_1, t_2) \tag{3.23}$$

$$\tag{3.24}$$

where we have the decay rate of particle a, the rate of the first decay and the second respectively. These obviously satisfy $\Gamma_a(t) = \frac{1}{2}(\Gamma_1(t) + \Gamma_2(t))$, being the two situations equiprobable. Both QM and hidden-variable theories predict that both kaons can be described by a decay rate equal to Γ_1, while after one particle decays the other's decay rate changes instantaneously to Γ_2. Yet, for our assumption of locality we must introduce a delay in this update. In particular, if t_1 is the proper time of the first particle at decay, the second one gets the information at time $t_1' = \frac{1+\beta}{1-\beta} t_1$. There are two main ways the experimental results could be misinterpreted, resulting in an overestimation of the analysed process:

- **CP violation:** The identification of the particles is based on the subsequent decays, namely $K_S \to \pi^+\pi^-$ and $K_L \to 3\pi$. The possible direct violation of CP gives rise to the process $K_L \to \pi^+\pi^-$, which we need to consider. In particular, the branching factor equals 1.96710^{-3}.
- **Regeneration:** A K_L could $transform$ into a K_S when interacting with matter, due to the different cross sections of its components. In Chapter 1 this phenomenon is explained in detail.

Considering these corrections, the experiments give contrasting results with a local theory. In particular, the BESIII collaboration found a cross section 2 orders of magnitude lower than expected [32].

CPT violation and decoherence

The previous analysis also enables the investigation of minute decoherence and CPT violation effects, which could be significant within the context of quantum gravity theories. Namely, fluctuations in the topology and metric at the Plank scale, i.e. space-time foam, could result in decoherence of the state, even when isolated. This has been shown to be in contrast with the CPT theorem. The relevant parameters can be obtained by fitting the distribution of time intervals between the decay of the two kaons [33].

Conclusions

In this thesis, I explored the phenomenon of quantum entanglement within the context of high-energy physics, focusing on its manifestation and detectability in particle physics experiments. Starting from a theoretical foundation, I drew the mathematical framework of quantum mechanics that allows for entangled states, and explained some basic concepts at the core of the Standard Model. I then transitioned to practical aspects, discussing how entanglement can be studied through specific processes observable at particle colliders, such as the Large Hadron Collider (LHC). Based on the papers reviewed, I can clearly state that the experiments at high energies have been found consistent with expectations. Entanglement appears to be a resilient feature of quantum mechanics, even in this context. Nevertheless, the study of this phenomenon in particle physics is just at its beginnings and new ideas and applications are emerging and need to be uncovered. Its relevance as a quantum probe into the fundamental forces remains a pivotal aspect of future research.

Bibliography

[1] E. Conte, B. Fuks, and G. Serret. Madanalysis 5, a user-friendly framework for collider phenomenology. *Comput. Phys. Commun.*, 184:222–256, 2013. doi: 10.1016/j.cpc.2012.09.009.

[2] J. Alwall, R. Frederix, S. Frixione, V. Hirschi, F. Maltoni, O. Mattelaer, H.-S. Shao, T. Stelzer, P. Torrielli, and M. Zaro. The automated computation of tree-level and next-to-leading order differential cross sections, and their matching to parton shower simulations. *Journal of High Energy Physics*, 2014(7), July 2014. ISSN 1029-8479. doi: 10.1007/jhep07(2014)079. URL `http://dx.doi.org/10.1007/JHEP07(2014)079`.

[3] B. Podolsky A. Einstein and N. Rosen. Can quantum-mechanical description of physical reality be considered complete? *Physical Review*, 47:777–780, 1935. doi: 10.1103/PhysRev.47.777.

[4] J. S. Bell. On the einstein podolsky rosen paradox. *Physics Physique Fizika*, 1:195–200, Nov 1964. doi: 10.1103/PhysicsPhysiqueFizika.1.195. URL `https://link.aps.org/doi/10.1103/PhysicsPhysiqueFizika.1.195`.

[5] J F Clauser and A Shimony. Bell's theorem. experimental tests and implications. *Reports on Progress in Physics*, 41(12):1881, dec 1978. doi: 10.1088/0034-4885/41/12/002. URL `https://dx.doi.org/10.1088/0034-4885/41/12/002`.

[6] John F. Clauser, Michael A. Horne, Abner Shimony, and Richard A. Holt. Proposed experiment to test local hidden-variable theories. *Phys. Rev. Lett.*, 23:880–884, Oct 1969. doi: 10.1103/PhysRevLett.23.880. URL `https://link.aps.org/doi/10.1103/PhysRevLett.23.880`.

[7] Yu Guo. The chsh-type inequalities for infinite-dimensional quantum systems. *arXiv preprint arXiv:1308.3287*, 2013.

[8] Daniel M. Greenberger, Michael A. Horne, Abner Shimony, and Anton Zeilinger. Bell's theorem without inequalities. *American Journal of Physics*, 58(12):1131–1143, 12 1990. ISSN 0002-9505. doi: 10.1119/1.16243. URL `https://doi.org/10.1119/1.16243`.

[9] B. S. Cirel'son. Quantum generalizations of bell's inequality. *Letters in Mathematical Physics*, 4: 93–100, 1980.

[10] Alain Aspect, Jean Dalibard, and Gérard Roger. Experimental test of bell's inequalities using time-varying analyzers. *Phys. Rev. Lett.*, 49:1804–1807, Dec 1982. doi: 10.1103/PhysRevLett.49.1804. URL `https://link.aps.org/doi/10.1103/PhysRevLett.49.1804`.

[11] B. Hensen, H. Bernien, A. E. Dréau, A. Reiserer, N. Kalb, M. S. Blok, J. Ruitenberg, R. F. L. Vermeulen, R. N. Schouten, C. Abellán, W. Amaya, V. Pruneri, M. W. Mitchell, M. Markham, D. J. Twitchen, D. Elkouss, S. Wehner, T. H. Taminiau, and R. Hanson. Loophole-free bell inequality violation using electron spins separated by 1.3 kilometres. *Nature*, 526(7575):682–686, 2015. ISSN 1476-4687. doi: 10.1038/nature15759. URL `https://doi.org/10.1038/nature15759`.

[12] Michael A. Nielsen and Isaac L. Chuang. *Quantum Computation and Quantum Information: 10th Anniversary Edition*. Cambridge University Press, 40 W. 20 St. New York, NY, United States, 2011. ISBN 978-1-107-00217-3.

[13] Ryszard Horodecki, Paweł Horodecki, Michał Horodecki, and Karol Horodecki. Quantum entanglement. *Rev. Mod. Phys.*, 81:865–942, Jun 2009. doi: 10.1103/RevModPhys.81.865. URL https://link.aps.org/doi/10.1103/RevModPhys.81.865.

[14] R. Horodecki, P. Horodecki, and M. Horodecki. Violating bell inequality by mixed spin-12 states: necessary and sufficient condition. *Physics Letters A*, 200(5):340–344, 1995. ISSN 0375-9601. doi: https://doi.org/10.1016/0375-9601(95)00214-N. URL https://www.sciencedirect.com/science/article/pii/037596019500214N.

[15] Willis E. Lamb. *Banquet speech*. Nobel Foundation, Stockholm, 1956. URL https://www.nobelprize.org/prizes/physics/1955/lamb/speech/.

[16] Abdus Salam. Weak and electromagnetic interactions. *Il Nuovo Cimento (1955-1965)*, 11:568–577, 1959. URL https://api.semanticscholar.org/CorpusID:15889731.

[17] Peter W. Higgs. Broken symmetries and the masses of gauge bosons. *Phys. Rev. Lett.*, 13:508–509, Oct 1964. doi: 10.1103/PhysRevLett.13.508. URL https://link.aps.org/doi/10.1103/PhysRevLett.13.508.

[18] Aad et al. Observation of a new particle in the search for the standard model higgs boson with the atlas detector at the lhc. *Physics Letters B*, 716(1):1–29, September 2012. ISSN 0370-2693. doi: 10.1016/j.physletb.2012.08.020. URL http://dx.doi.org/10.1016/j.physletb.2012.08.020.

[19] David Griffiths. *Introduction to Elementary Particles*. John Wiley Sons, 2008. ISBN 978-3-527-61847-7.

[20] Nahid Binandeh Dehaghani, A. Pedro Aguiar, and Rafal Wisniewski. Exploring strange entanglement: Experimental and theoretical perspectives on neutral kaon systems, 2023.

[21] Antonio Di Domenico. Entanglement, cpt and neutral kaons, 2022.

[22] Fabio Maltoni, Claudio Severi, Simone Tentori, and Eleni Vryonidou. Quantum detection of new physics in top-quark pair production at the lhc, 2024.

[23] Zhongtian Dong, Dorival Gonçalves, Kyoungchul Kong, and Alberto Navarro. When the machine chimes the bell: Entanglement and bell inequalities with boosted $t\bar{t}$, 2024.

[24] Claudio Severi, Cristian Degli Esposti Boschi, Fabio Maltoni, and Maximiliano Sioli. Quantum tops at the lhc: from entanglement to bell inequalities. *The European Physical Journal C*, 82(4), April 2022. ISSN 1434-6052. doi: 10.1140/epjc/s10052-022-10245-9. URL http://dx.doi.org/10.1140/epjc/s10052-022-10245-9.

[25] Marco Fabbrichesi, Roberto Floreanini, and Emidio Gabrielli. Constraining new physics in entangled two-qubit systems: top-quark, tau-lepton and photon pairs. *The European Physical Journal C*, 83(2), February 2023. ISSN 1434-6052. doi: 10.1140/epjc/s10052-023-11307-2. URL http://dx.doi.org/10.1140/epjc/s10052-023-11307-2.

[26] Alan J. Barr, Marco Fabbrichesi, Roberto Floreanini, Emidio Gabrielli, and Luca Marzola. Quantum entanglement and bell inequality violation at colliders, 2024.

[27] Yoav Afik and Juan Ramón Muñoz de Nova. Entanglement and quantum tomography with top quarks at the lhc. *The European Physical Journal Plus*, 136(9):907, 2021. ISSN 2190-5444. doi: 10.1140/epjp/s13360-021-01902-1. URL https://doi.org/10.1140/epjp/s13360-021-01902-1.

[28] ATLAS Collaboration. Observation of quantum entanglement in top-quark pairs using the atlas detector, 2023.

[29] J.A. Aguilar-Saavedra, A. Bernal, J.A. Casas, and J.M. Moreno. Testing entanglement and bell inequalities in h $\to$ z z. *Physical Review D*, 107(1), January 2023. ISSN 2470-0029. doi: 10.1103/physrevd.107.016012. URL http://dx.doi.org/10.1103/PhysRevD.107.016012.

[30] A. Acín, T. Durt, N. Gisin, and J. I. Latorre. Quantum nonlocality in two three-level systems. *Physical Review A*, 65(5), May 2002. ISSN 1094-1622. doi: 10.1103/physreva.65.052325. URL http://dx.doi.org/10.1103/PhysRevA.65.052325.

[31] Pei-Cheng Jiang, Xuan Wang, and Da-Yong Wang. Test of quantum nonlocality via vector meson decays to ksks. *International Journal of Modern Physics A*, 36(26), September 2021. ISSN 1793-656X. doi: 10.1142/s0217751x21501785. URL http://dx.doi.org/10.1142/S0217751X21501785.

[32] Ablikim et al. Branching fraction measurement of $j/\psi \to K_S K_L$ and search for $j/\psi \to K_S K_S$. *Phys. Rev. D*, 96:112001, Dec 2017. doi: 10.1103/PhysRevD.96.112001. URL https://link.aps.org/doi/10.1103/PhysRevD.96.112001.

[33] D. Babusci et al. Precision tests of quantum mechanics and cpt symmetry with entangled neutral kaons at kloe, 2022.